Accessing mixed cluster rare-earth MOFs with reduced connectivity via linker expansion and desymmetrization: co-assembly of 6-c and 10-c hexanuclear clusters in RE-stc-MOF-1

Edward Loukopoulos,[a] Constantinos Tsangarakis,[a] Konstantinos G. Froudas,[a] Maria Vassaki,[a] Giasemi K. Angeli[a,b] and Pantelis N. Trikalitis*[a]

[a] Department of Chemistry, University of Crete, 71003 Heraklion, Greece
[b] Theoretical and Physical Chemistry Institute, National Hellenic Research Foundation, 48 Vassileos Constantinou Avenue, Athens, 11635 Greece

SUPPORTING INFORMATION

Table of contents

Methods and Instrumentation

Materials. H_4**L** was synthesized as detailed in pages S5-S7. All chemicals were purchased commercially and were used without further purification. HCl (37%), $Pd(PPh_3)_4$, H_2SO_4, acetone (99.5%), CH_2Cl_2 (> 99.9%), THF (>99.9%), methanol (>99.8%), ethanol absolute, NaOH (98%, pellets), N,N-dimethylformamide (DMF, 99.8%), and potassium disulfate were purchased from Aldrich. 1,3,5-tribromobenzene, $Y(NO_3)_3{\cdot}6H_2O$ 99.9%, $Sm(NO_3)_3{\cdot}6H_2O$ 99.9%, $Eu(NO_3)_3{\cdot}6H_2O$ 99.9%, $Dy(NO_3)_3{\cdot}5H_2O$ 99.9%, $Tb(NO_3)_3{\cdot}6H_2O$ 99.9% and boronic acid were purchased from Alfa Aesar. 2-fluorobenzoic acid was purchased from Fluorochem.

NMR spectroscopy: ^{1}H- and ^{19}F-NMR spectra were recorded on a 500MHz Bruker spectrometer. MOF samples were prepared by digesting a small portion (~2 mg) of the solids (as-made or activated) with a drop of concentrated HCl (37%) in a DMSO-d_6 solution. Chemical shifts are quoted in parts per million (ppm). Data were analysed and visualised using the softwares TopSpin 3.6.4 and MestReNova 12.

Powder X-Ray Diffraction (PXRD): PXRD patterns were collected using a Rigaku SmartLab System Cu Kα (λ = 1.5418 A) radiation operating at 40 kV and 50 mA. A typical scan rate was 1.5 deg (o)/min with a step size of 0.02 deg. Calculated PXRD patterns from the corresponding single-crystal data of Eu-**stc**-MOF-1 were obtained using Mercury 3.8.[1]

Single Crystal X-ray Diffraction (SCXRD): SCXRD data were collected on a Bruker D8 Venture diffractometer equipped with a Cu Incoatec microfocus IμS 3.0 source, a Photon II detector operating in shutterless mode and a cryostream 800 system (Oxford Cryosystems) for temperature regulation.

Scanning Electron Microscope (SEM): Images were obtained using a JEOL JSM-IT700HR microscope.

Sample activation and gas sorption measurements. Low pressure N_2 and Ar gas sorption measurements were carried at different temperatures up to 1 bar using a Quantachrome Autosorb-iQ2 instrument equipped with a cryocooler system capable of temperature control from

20 to 320 K. Prior to analysis, the as-made samples were washed with DMF three times per day for 3 days to remove any unreacted starting materials from the pores. The DMF solvent was then replaced with fresh ethanol solution (3 ml) two times per day for 6 days. The absence of DMF molecules was further confirmed by ^{1}H-NMR spectroscopy.

Direct activation using vacuum**.** An ethanol exchanged sample was transferred to a 9 mm sample cell and activated under dynamic vacuum at a selected temperature (25, 40 or 80 ^{o}C) for 16 hours until the outgas rate was less than 2 mTorr/min. After the evacuation, the sample was re-weighed to obtain the precise mass of the sample and the cell was transferred to the analysis port of the gas sorption instrument.

Supercritical CO_2 activation ($scCO_2$): A home build $scCO_2$ activation apparatus was used, operating under flow conditions, similar to the system reported by Matzger and co-workers.[2] After activation the sample was transferred inside an Argon filled glove box, loaded into a 9 mm sample cell, weighted and transferred to the analysis port of the gas sorption instrument.

Thermogravimetric analysis (TGA) measurements were performed using a TA Instrument TGA 5500. An amount of approximately 10 mg of activated RE-stc-MOF-1 (RE: Eu and Tb) was placed inside a quartz cap and heated up to 850 ^{o}C under N_2 flow with a heating rate of 5 ^{o}C/min.

Organic synthesis and ^{1}H NMR spectra

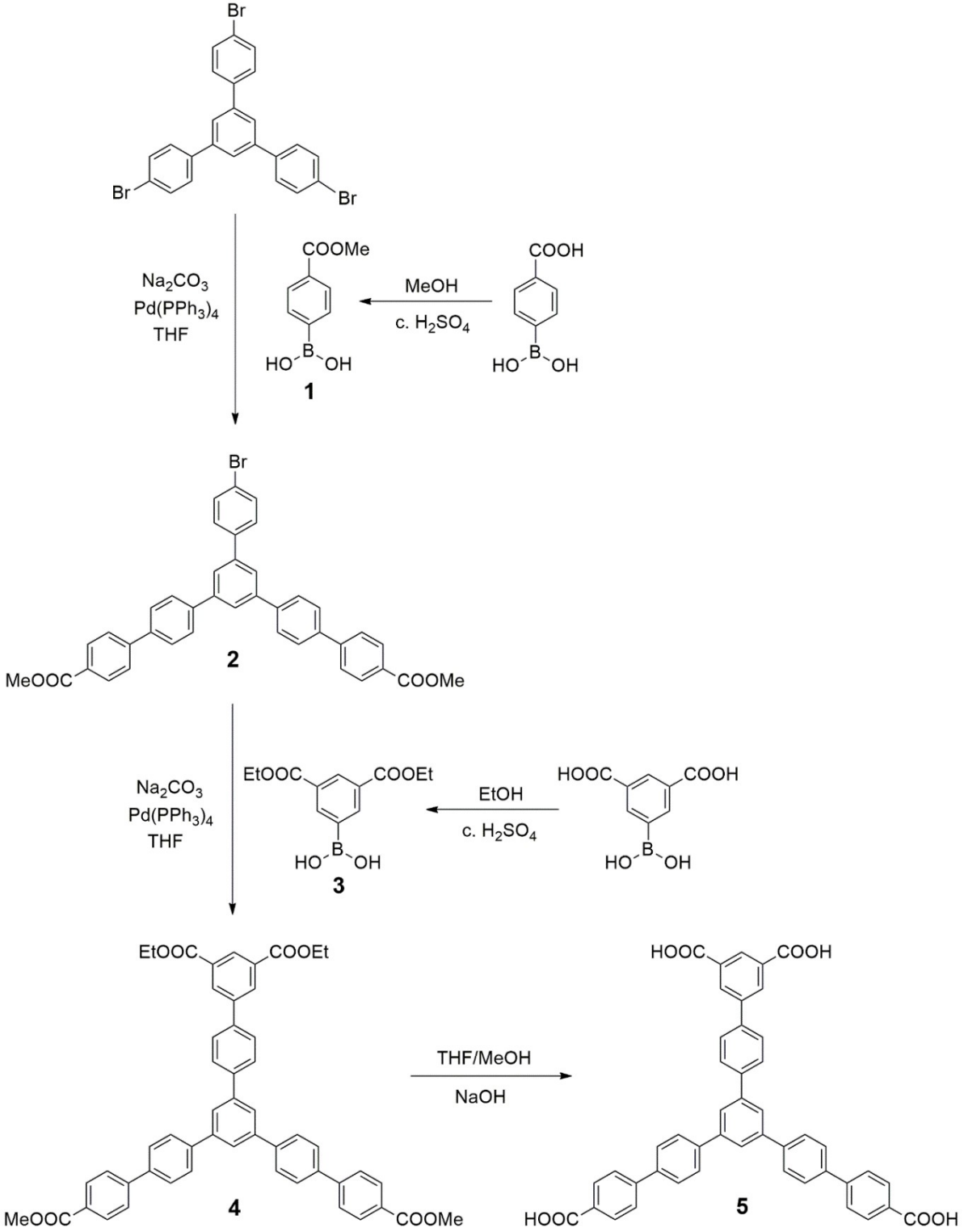

Scheme S1. Synthesis of the organic ligand H_4**L** (**5**). IUPAC name: 5''-(4'-carboxy-[1,1'-biphenyl]-4-yl)-[1,1':4',1'':3'',1''':4''',1''''-quinquephenyl]-3,4''',5-tricarboxylic acid.

Preparation of compounds 1 and 3 was performed as previously reported.[3]

Preparation of compound 2. A dried under Ar double neck round-bottom flask was filled with 0.33 g (1.84 mmol) of compound **1**, 0.5 g (0.92 mmol) of 1,3,5-tris(4-bromophenyl)benzene, 30 ml dry THF, 10 ml Na_2CO_3 2 M and 45 mg $Pd(PPh_3)_4$. The mixture was refluxed at 80 ^oC under Ar atmosphere for 2 days. Upon cooling to room temperature, the reaction mixture was extracted with THF which was then removed through rotary evaporation. The crude residue was purified through column chromatography on silica gel with petroleum ether/dichloromethane mixture (4:1 v/v) as an eluent, to produce a white solid.

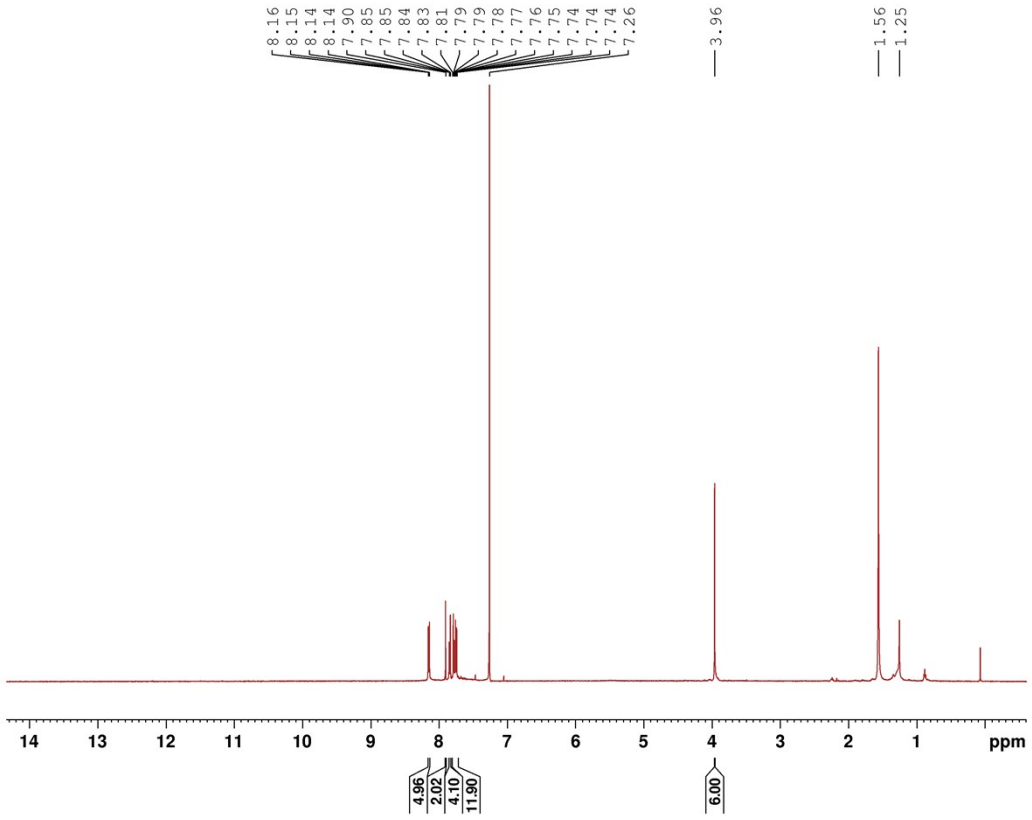

Figure S1. ^{1}H-NMR spectrum of compound **2** in $CDCl_3$ (500MHz).

Preparation of compound 4. A dried under Ar double neck round-bottom flask was filled with 0.15 g (0.23 mmol) of compound **2**, 0.122 g (0.46 mmol) of compound **3**, 20 ml dry THF, 5 ml Na_2CO_3 2 M and 35 mg $Pd(PPh_3)_4$. The mixture was refluxed at 80 ^oC under Ar atmosphere for 3 days. Upon cooling to room temperature, the reaction mixture was extracted with THF which

was then removed through rotary evaporation. The crude residue was purified through column chromatography on silica gel with hexane/ethyl acetate mixture (2:1 v/v) as an eluent, to produce a white solid.

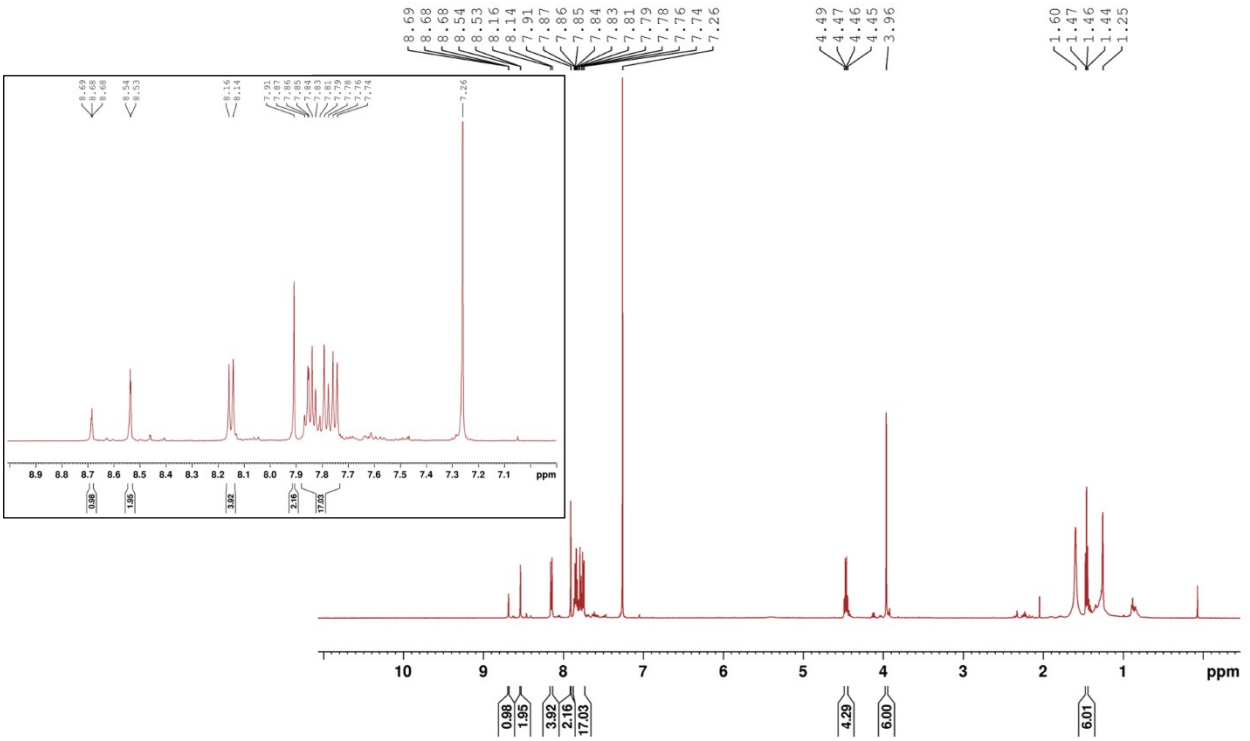

Figure S2. ^{1}H-NMR spectrum of compound **4** in $CDCl_3$ (500MHz). Inset shows the region of aromatic protons in more detail.

Preparation of compound 5. A mixture containing 0.2 g (0.25 mmol) of compound **4**, 10 ml THF, 10 ml MeOH and 10 ml NaOH 5 N was refluxed at 80 ^{o}C overnight. Upon cooling to room temperature, the mixture was acidified with 3N HCl to produce a white solid. The solid was filtrated, washed copiously with water and dried to afford the product without any further purification.

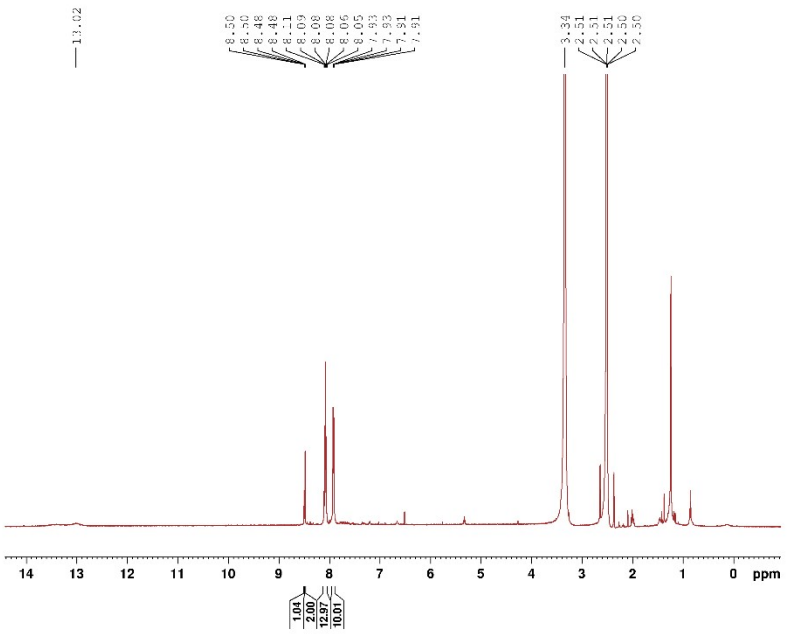

Figure S3. ^{1}H-NMR spectrum of compound **5** in DMSO-d_6 (500MHz).

MOF Synthesis

Synthesis of Y-**stc**-MOF-1**.** $Y(NO_3)_3 \cdot 6H_2O$ (13.7 mg, 0.036 mmol), 2-fluorobenzoic acid (200 mg, 1.43 mmol), H_2O (0.15 ml) and H_4**L** (6.4 mg, 0.009 mmol) were added to a 3 ml solution of DMF, which was then transferred to a 20 ml glass scintillation vial. The vial was sealed and placed in an isothermal oven at 120 ^{o}C for 48 hours. During that period, polyhedral crystals were formed. (30% yield based on H_4**L**).

Synthesis of Sm-**stc**-MOF-1**.** The same synthetic protocol was employed as described above, with $Sm(NO_3)_3 \cdot 6H_2O$ (16.0 mg, 0.036 mmol) as the metal salt. The vial containing the reaction mixture was sealed and placed in an isothermal oven at 120 ^{o}C for 24 hours. During that period, polyhedral crystals were formed. (25% yield based on H_4**L**).

Synthesis of Eu-**stc**-MOF-1**.** The same method was employed as described above, with $Eu(NO_3)_3 \cdot 6H_2O$ (16.1 mg, 0.036 mmol) as the metal salt. The vial containing the reaction mixture was sealed and placed in an isothermal oven at 120 ^{o}C for 24 hours. During that period, polyhedral crystals were formed. (45% yield based on H_4**L**).

Synthesis of Tb-**stc**-MOF-1**.** The same method was employed as described above, with $Tb(NO_3)_3 \cdot 6H_2O$ (16.3 mg, 0.036 mmol) as the metal salt. The vial containing the reaction mixture was sealed and placed in an isothermal oven at 120 °C for 24 hours. During that period, polyhedral crystals were formed. (45% yield based on H_4**L**).

Synthesis of Dy-**stc**-MOF-1**.** The same method was employed as described above, with $Dy(NO_3)_3 \cdot 5H_2O$ (15.8 mg, 0.036 mmol) as the metal salt. The vial containing the reaction mixture was sealed and placed in an isothermal oven at 120 °C for 48 hours. During that period, polyhedral crystals were formed. (30% yield based on H_4**L**).

Table S1. Synthetic screening for the optimal conditions to obtain RE-**stc**-MOF-1.

Entry	**Metal: Ligand ratio**	**Solvent(s)**	**Modulator**	**Temp. (°C)**	**Result**
1	1:1	DMF	2-FBA (200 mg)	120	No solid
2		DMF : H_2O (4 : 1)			No solid
3	2:1	DMF	2-FBA (200 mg)		No solid
4		DMF : H_2O (4 : 1)			White amorphous solid
5	4:1	DMF	2-FBA (200 mg)		White amorphous solid
6		DMF : H_2O (4 : 1)	2-FBA (200 mg)		Colourless single crystals and white amorphous solid
7			2-FBA (100 mg)		Colourless single crystals and white amorphous solid
8			2-FBA (300 mg)		Colourless single crystals and white amorphous solid
9			2-FBA (400 mg)		White amorphous solid
10			2-FBA (200 mg) HCOOH (0.15 ml)		Colourless single crystals and white amorphous solid
11			HCOOH (0.15 ml)		No solid
12			CH_3COOH (0.15 ml)		No solid
13			2-FBA (200 mg) CH_3COOH (0.15 ml)		Colourless single crystals and white amorphous solid
14			Benzoic Acid (200 mg)		No solid
13		DMF : H_2O (3.2 : 1)			White amorphous solid

14		DMF : H_2O (2.5 : 1)	2-FBA (200 mg)		White amorphous solid
15		DMF : H_2O (2 : 1)			White amorphous solid
16		DMF : H_2O (2 : 1)	2-FBA (400 mg)		White amorphous solid
17		DMF : H_2O (6 : 1)	2-FBA (200 mg)		Colourless single crystals and white amorphous solid
18		DMF : H_2O (10 : 1)			Colourless single crystals and white amorphous solid
19		DMF : H_2O (15 : 1)			Colourless single crystals and white amorphous solid
20		DMF : H_2O (20 : 1)			Colourless single crystals

NMR spectra of acid digested samples

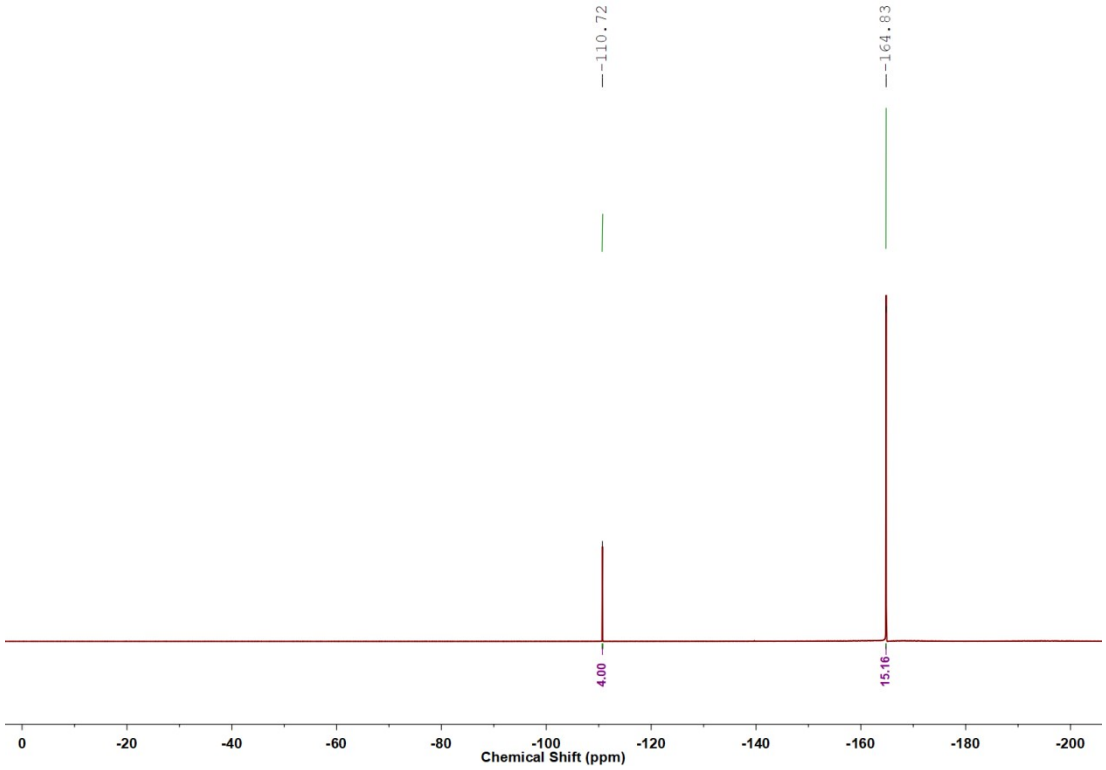

Figure S4. ^{19}F-NMR spectrum of Y-**stc**-MOF-1 (digested in HCl/DMSO-d_6 solution). The integration for both fluorine species indicates the average presence of 7.58 F^- anions per RE_6 cluster.

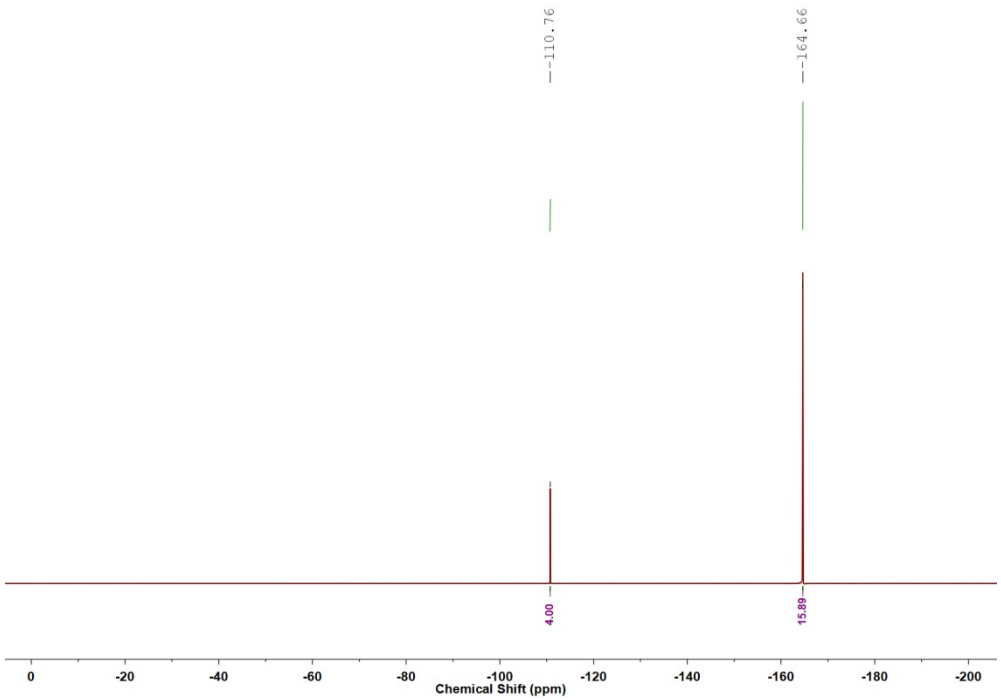

Figure S5. ^{19}F-NMR spectrum of Sm-**stc**-MOF-1 (digested in HCl/DMSO-d_6 solution). The integration for both fluorine species indicates the average presence of 7.94 F^- anions per RE_6 cluster.

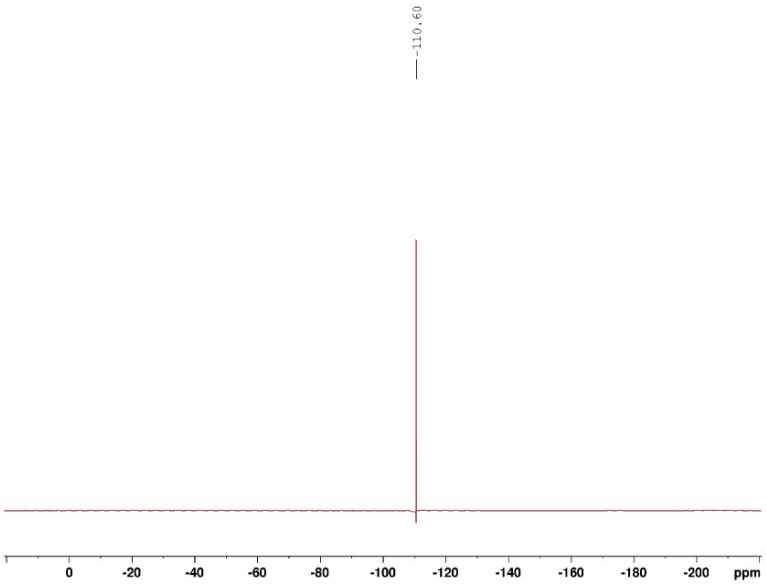

Figure S6. Reference ^{19}F-NMR spectrum of 2-fluorobenzoic acid (in DMSO-d_6 solution).

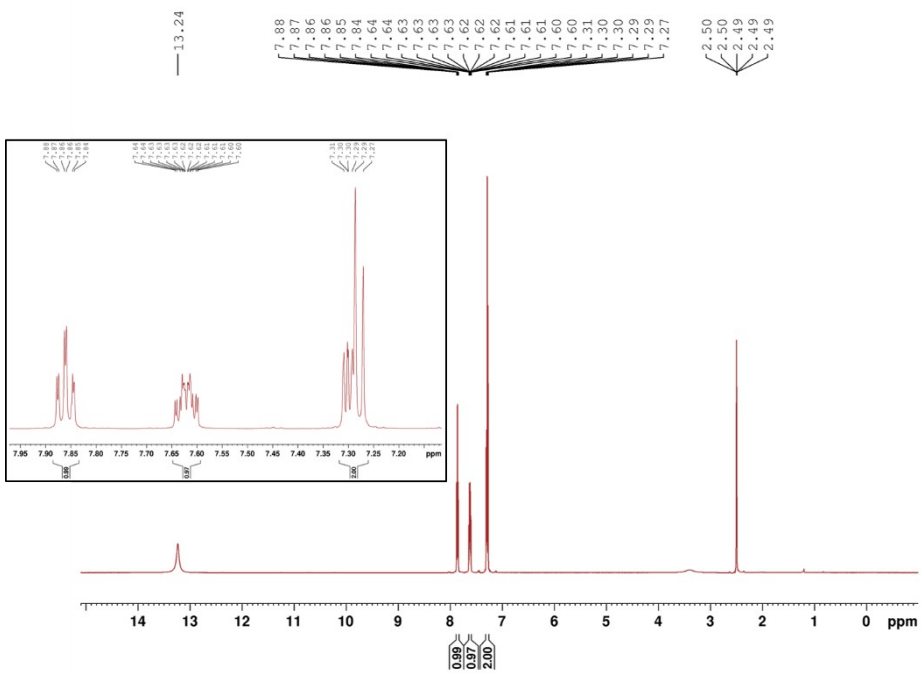

Figure S7. Reference [1]H-NMR spectrum of 2-fluorobenzoic acid (in DMSO-d_6 solution). Inset shows the region of aromatic protons in more detail.

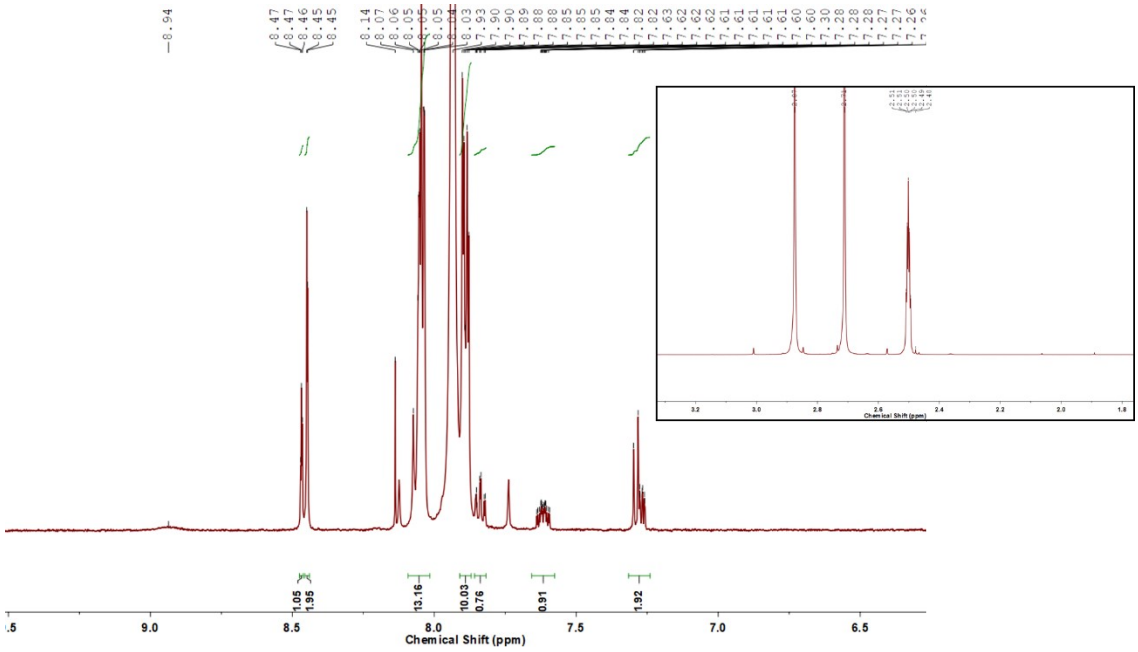

Figure S8. [1]H-NMR spectrum of as-made Y-**stc**-MOF-1 (digested in HCl/DMSO-d_6 solution). The ratio between ligand:FBA molecules was estimated at 1:1. The peaks at 2.73, 2.87 and 7.93 correspond to DMF (additional satellite peaks at 7.74 and 8.13 ppm), and the signal at 8.14

corresponds to formic acid (due to DMF decomposition). The dimethylammonium cation peaks were located at 2.48 and 8.94 ppm, in agreement with the literature,[4] but could not be reliably integrated due to respective DMSO peak overlap and broad -NH_2 signal respectively.

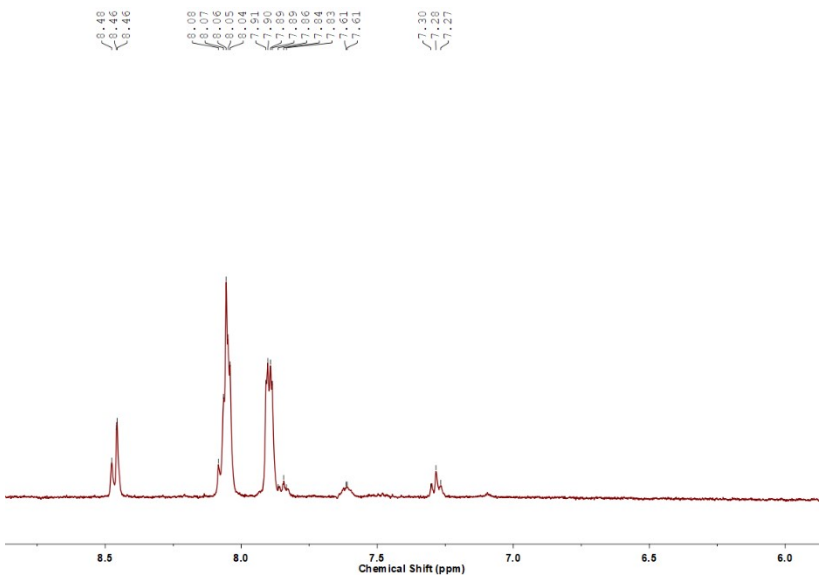

Figure S9. ^{1}H-NMR aromatic region spectrum of EtOH-exchanged Tb-**stc**-MOF-1 (digested in HCl/DMSO-d_6 solution), confirming the absence of signals related to DMF.

Single crystal X-ray crystallography and structural figures

The structures of Eu-**stc**-MOF-1 and Sm-**stc**-MOF-1 were determined using OLEX2,[5] solved using SHELXT[6] and refined with SHELXL-2014.[7] Both structures display large voids filled with heavily disordered counterions ($[NH_2(CH_3)_2]^{2+}$) and residual solvent (DMF) molecules. For these reasons, certain restraints/constraints in regards to distance, geometry, planarity and ADPs have been used to retain chemical feasibility in the model. Additionally, in Sm-**stc**-MOF-1 we were unable to model the entire 2-fluorobenzoate moieties, due to weak crystal diffraction. In this case, only the respective carboxyl groups were modelled. Efforts to further improve crystal quality proved unsuccessful, however the presence of 2-fluorobenzoates was confirmed through ^{19}F-NMR studies (see the NMR section of the SI). The contribution of non-modelled fluorobenzoates and disordered counterions/solvent molecules was treated as diffuse using the solvent mask routine implemented in the OLEX2 interface.[5] All non-H atoms were refined with

anisotropic thermal parameters. H-atoms were introduced at calculated positions and allowed to ride on their carrier atoms.

Moreover, in both structures the μ_3-X (X = OH^- or F^-) groups were refined using as both hydroxo- and fluoro-groups and the dataset with improved and most feasible crystallographic parameters (e.g., by comparing the related U_{eq} parameter values compared to the ones of the neighbouring metal centres) was chosen in each case. Previous studies[3b, 8] have shown that mixed OH^- /F^- clusters typically form in such RE-MOFs, with composition that varies from crystal to crystal. As a result, SCXRD cannot provide irrefutable proof of the actual cluster formula and can only be suggestive of its composition. Results of the NMR section also support this observation.

Crystal data and structure refinement parameters for Eu-**stc**-MOF-1 and Sm-**stc**-MOF-1 are given in Tables S2-S3 (CCDC: 2374028-2374029). Additional geometric/crystallographic calculations were performed using PLATON[9].

Table S2. Crystal data of Eu-**stc**-MOF-1, as made in DMF**.**

Identification code	Eu-**stc**-MOF-1
Empirical formula	$C_{118}H_{88}Eu_6F_{10}N_4O_{26}$
Formula weight	3079.68
Temperature/K	199.99
Crystal system	triclinic
Space group	P-1
a/Å	24.354(8)
b/Å	25.255(8)
c/Å	26.050(7)
α/°	79.367(9)
β/°	88.674(9)
γ/°	62.912(9)
Volume/Å^3	13986(7)
Z	2
ρ_{calc}g/cm^3	0.731
μ/mm^{-1}	1.362
F(000)	3000.0
Crystal size/mm^3	0.012 × 0.01 × 0.005
Radiation	MoKα (λ = 0.71073)
2θ range for data collection/°	4.366 to 44.228
Index ranges	$-25 \leq h \leq 25$, $-26 \leq k \leq 26$, $-27 \leq l \leq 27$
Reflections collected	163687

Independent reflections	34254 [R_{int} = 0.1634, R_{sigma} = 0.1301]
Data/restraints/parameters	34254/24/633
Goodness-of-fit on F^2	0.994
Final R indexes [I>=2σ (I)]	R_1 = 0.0944, wR_2 = 0.2471
Final R indexes [all data]	R_1 = 0.1205, wR_2 = 0.2677
Largest diff. peak/hole / e $Å^{-3}$	8.81/-1.67

Table S3. Crystal data of Sm-**stc**-MOF-1, as made in DMF**.**

Identification code	Sm-**stc**-MOF-1
Empirical formula	$C_{94}H_{52}F_8O_{26}Sm_6$
Formula weight	2651.45
Temperature/K	214.99
Crystal system	triclinic
Space group	P-1
a/Å	24.216(8)
b/Å	25.257(7)
c/Å	26.243(8)
α/°	77.829(15)
β/°	87.412(16)
γ/°	63.578(14)
Volume/$Å^3$	14029(8)
Z	2
$\rho_{calc}g/cm^3$	0.628
μ/mm^{-1}	9.530
F(000)	2548.0
Crystal size/mm^3	0.04 × 0.03 × 0.02
Radiation	CuKα (λ = 1.54178)
2θ range for data collection/°	4.08 to 102.394
Index ranges	$-24 \leq h \leq 23$, $-25 \leq k \leq 25$, $-26 \leq l \leq 26$
Reflections collected	62716
Independent reflections	28652 [R_{int} = 0.0674, R_{sigma} = 0.1032]
Data/restraints/parameters	28652/2/856
Goodness-of-fit on F^2	1.046
Final R indexes [I>=2σ (I)]	R_1 = 0.0701, wR_2 = 0.19461
Final R indexes [all data]	R_1 = 0.1056, wR_2 = 0.2332
Largest diff. peak/hole / e $Å^{-3}$	2.07/-2.48

Table S4. Characterization of strong C-H···π interactions in Eu-**stc**-MOF-1 (Cg = ring centroid).

C–H···ring	C–Cg distance [Å]	H–Cg distance [Å]	Perpendicular H–Cg distance [Å]	C–H–Cg angle[˚]
C10-H10···**A**^{i}	3.6469(12)	2.87	2.84	139.0(4)
C118-H11C···**B**^{i}	3.6681(12)	2.75	2.69	156.0(4)
C85-H85···**C**^{i}	3.5288(12)	2.93	2.75	122.0(4)

Rings: **A**: C67-C68-C69-C70-C71-C72, **B**: C73-C74-C75-C76-C77-C78, **C**: C14-C15-C16-C17-C18-C19

Symmetry codes: ^{i}: x, y, z, ^{ii}: 1-x, 2-y, -z.

Topological analysis considering the <u>4-c organic linker as two interconnected 3-c building units</u>

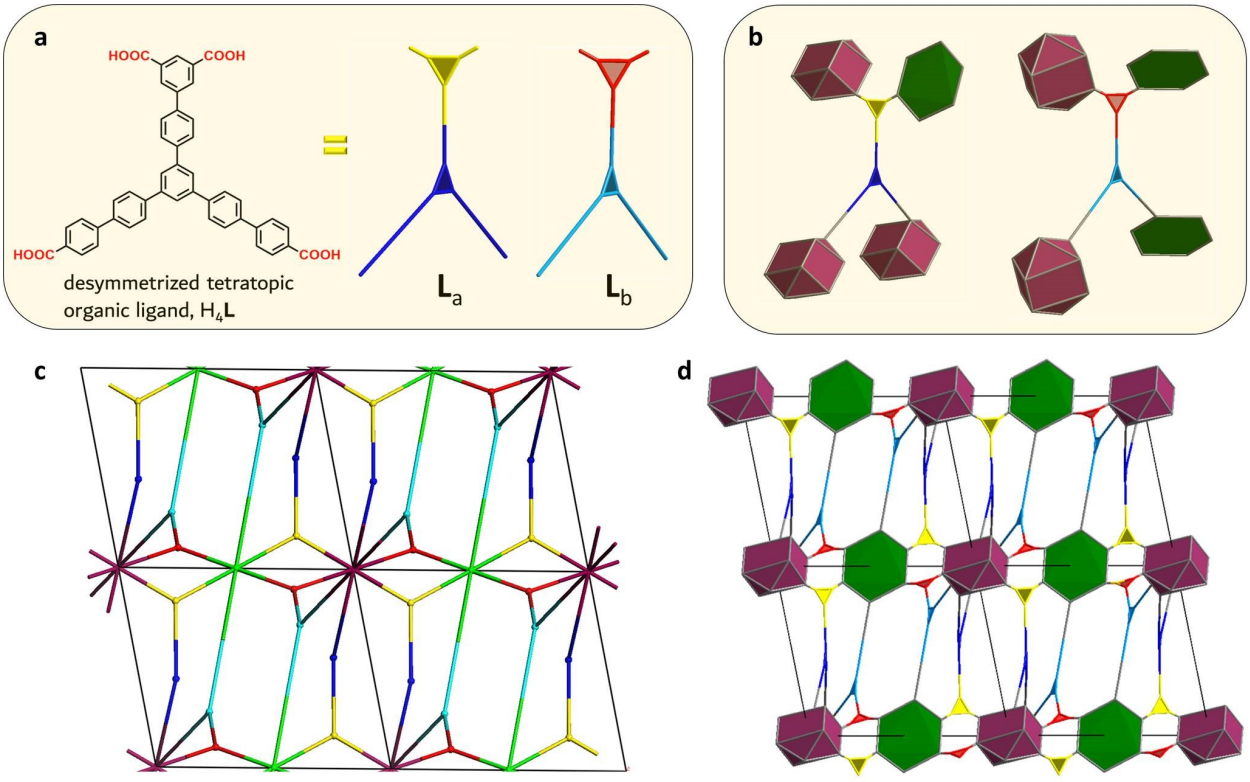

Figure S10. a) For the topological analysis of Eu-**stc**-MOF-1 the 4-connected $\mathbf{L}^{4-}$ organic linker is best described as two interconnected 3-c building units and there are two crystallogaphically distinct linkers denoted as $\mathbf{L_a}$ (yellow and **blue**) and $\mathbf{L_b}$ (**red** and **light blue**). b) The connectivity of the $\mathbf{L_a}$ and $\mathbf{L_b}$ linkers with the 6-c and 10-c SBUs. c) The derived non-augmented **stc** and d) the augmented **stc-a** (3,3,3,3,6,10)-c hexanodal net. The simplified non-augmented **stc** net (c) is obtained by reducing the $\mathbf{L_a}$ and $\mathbf{L_b}$ to the corresponding interconnected distinct 3-c nodes, as shown in (a), while the 6-c and 10-c Eu_6-clusters, to 6-c **green** and 10-c **dark red** nodes. The resulting 6-nodal **stc** net has a connectivity of (3,3,3,3,6,10)-c.

The topological analysis results are summarized below:

TD10=1560

Vertex symbols for selected sublattice

10-c dark red node Point symbol:{4^4.5^8.6^6.7^4.8^14.9^2.10^7}

Extended point symbol:

[4.4.4.4.5.5.5.5.5.5.5(2).5(2).6.6.6.6.6.6.7.7.7(2).7(2).8.8.8(2).8(2).8(2).8(2).8(2).8(2).8(2).8(2).8(2).8(2).8(3).8(3).9(2).9(2).10(2).10(4).10(4).10(8).10(8).10(8).10(8)]

6-c green node Point symbol:{4^2.5^2.6^2.7^2.8^4.9.10^2}

Extended point symbol:[4.4.5.5.6.6.7(2).7(2).8(2).8(2).8(4).8(4).9(4).10(8).10(12)]

3-c yellow node Point symbol:{4.5.6}

Extended point symbol:[4.5.6(2)]

3-c blue node Point symbol:{4.5.6}

Extended point symbol:[4.5.6(2)]

3-c red node Point symbol:{4.5.6}

Extended point symbol:[4.5(2).6]

3-c light blue node Point symbol:{5^2.6}

Extended point symbol:[5.5(2).6(2)]

Point symbol for net: {4.5.6}6{4^2.5^2.6^2.7^2.8^4.9.10^2}{4^4.5^8.6^6.7^4.8^14.9^2.10^7}{5^2.6}2

3,3,3,3,6,10-c net with stoichiometry (3-c)2(3-c)2(3-c)2(3-c)2(6-c)(10-c); **6-nodal net**

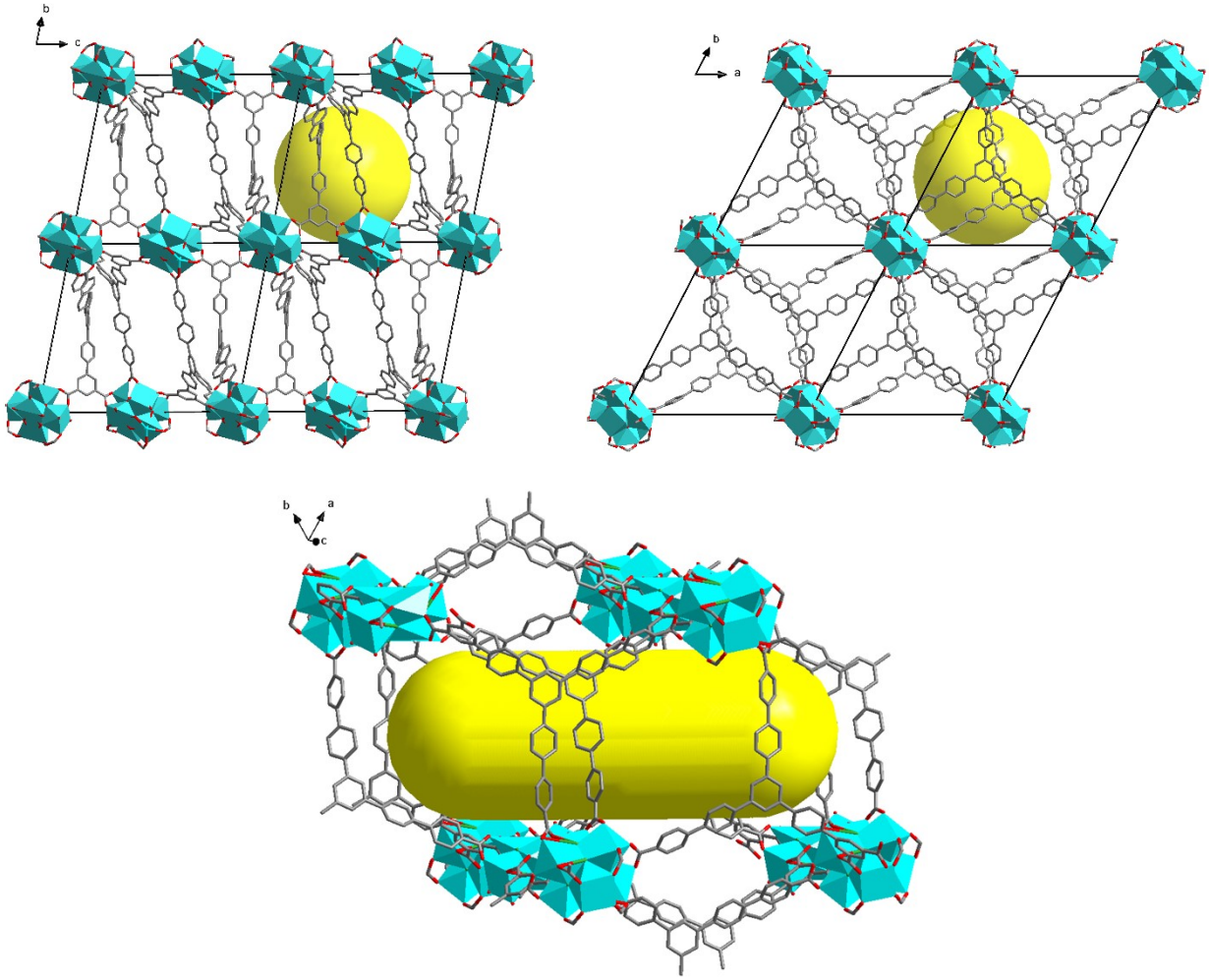

Figure S11. The location of the porous cavity in Eu-**stc**-MOF-1, looking down to *a* (left) and *c* (right) axis. The isolated elongated cavity is shown at the bottom.

Powder X-ray diffraction measurements

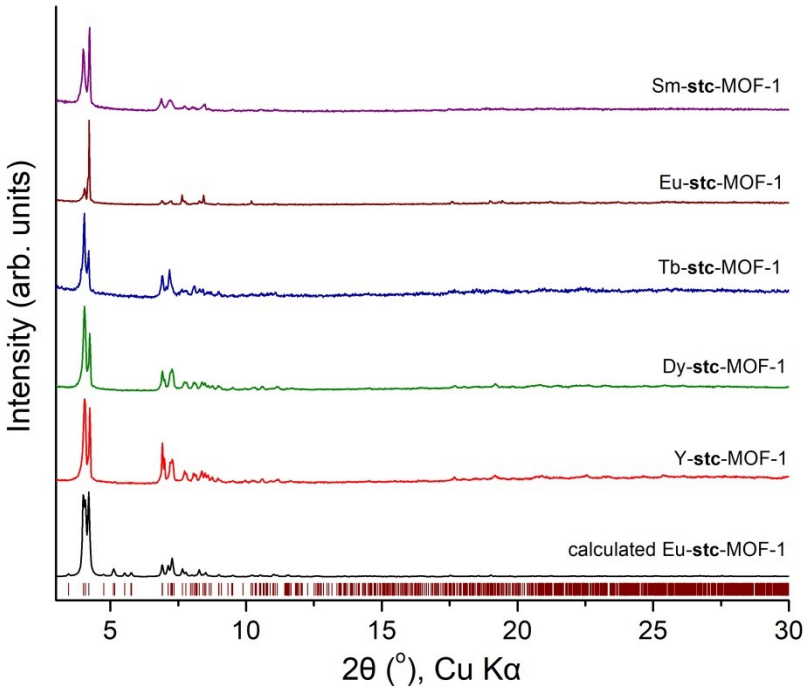

Figure S12. Experimental PXRD patterns of the as-made RE-**stc**-MOF series along with the calculated pattern obtained from the structure of Eu-**stc**-MOF-1.

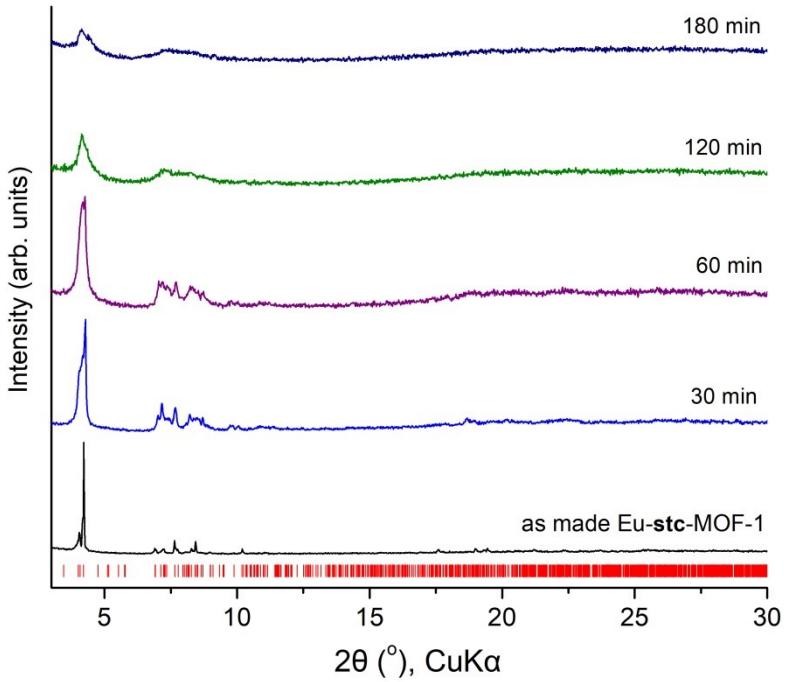

Figure S13. Experimental PXRD patterns of Eu-**stc**-MOF-1 in DMF, exposed in air atmosphere for various periods of time.

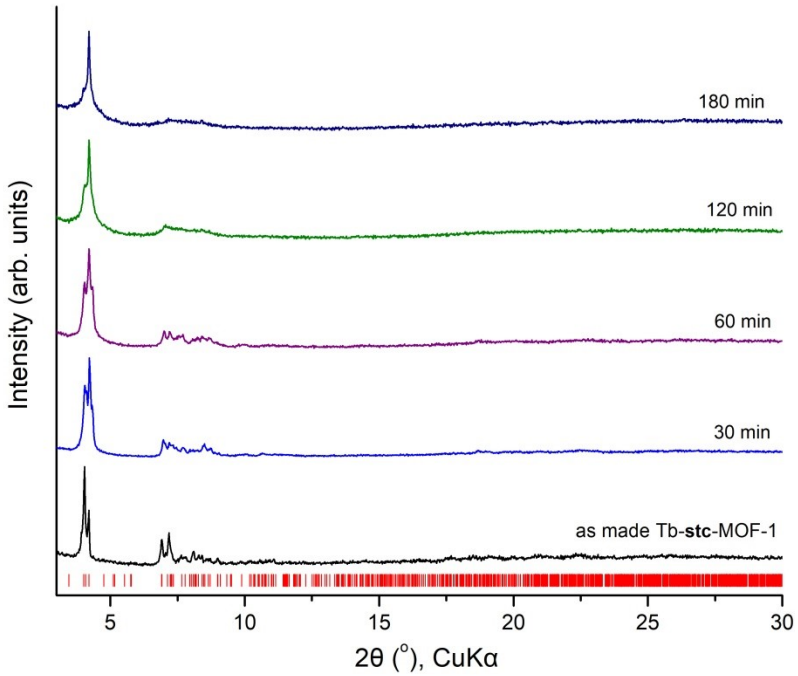

Figure S14. Experimental PXRD patterns of Tb-**stc**-MOF-1 in DMF, exposed in air atmosphere for various periods of time.

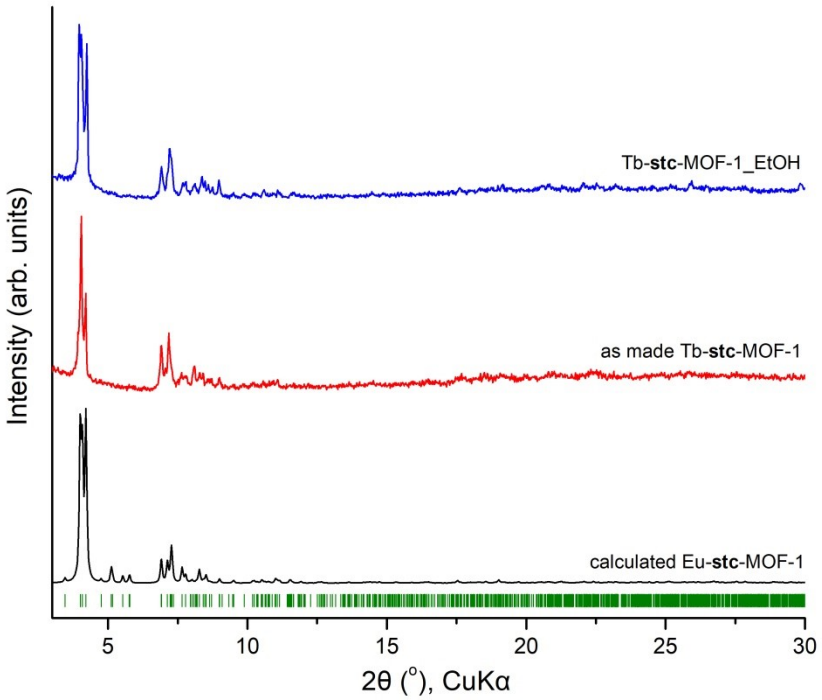

Figure S15. Experimental PXRD patterns of as-made Tb-**stc**-MOF-1 (red) and the corresponding ethanol exchanged sample (blue). The calculated pattern from the isostructural Eu-**stc**-MOF-1 compound is shown for comparison purposes (black).

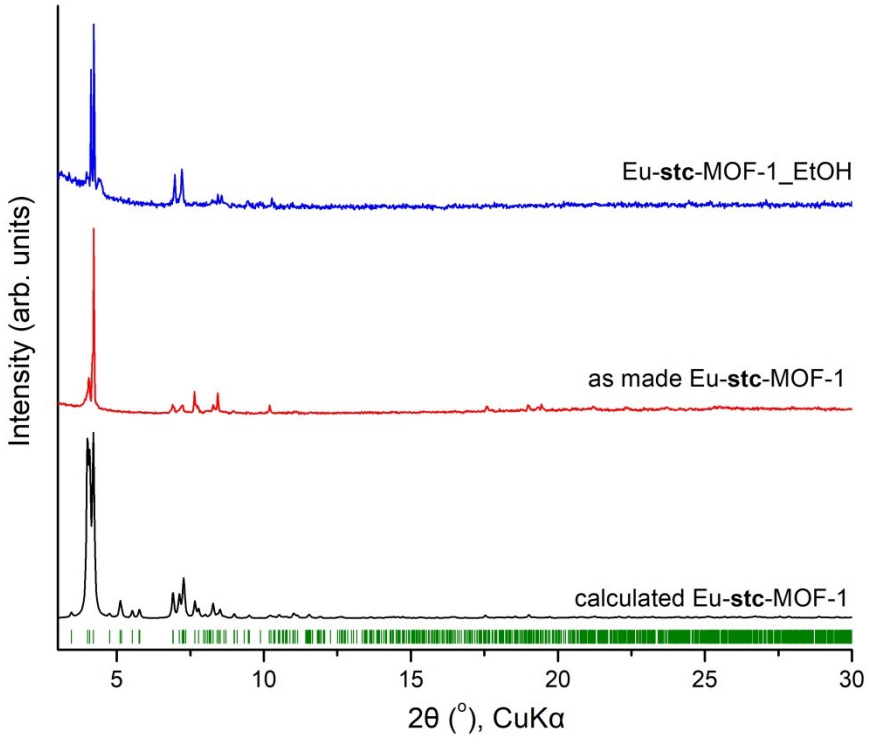

Figure S16. Experimental PXRD patterns of as-made Eu-**stc**-MOF-1 (red) and the corresponding ethanol exchanged sample (blue). The corresponding calculated pattern from the single crystal structure is shown for comparison purposes (black).

Scanning Electron Microscopy (SEM) Images

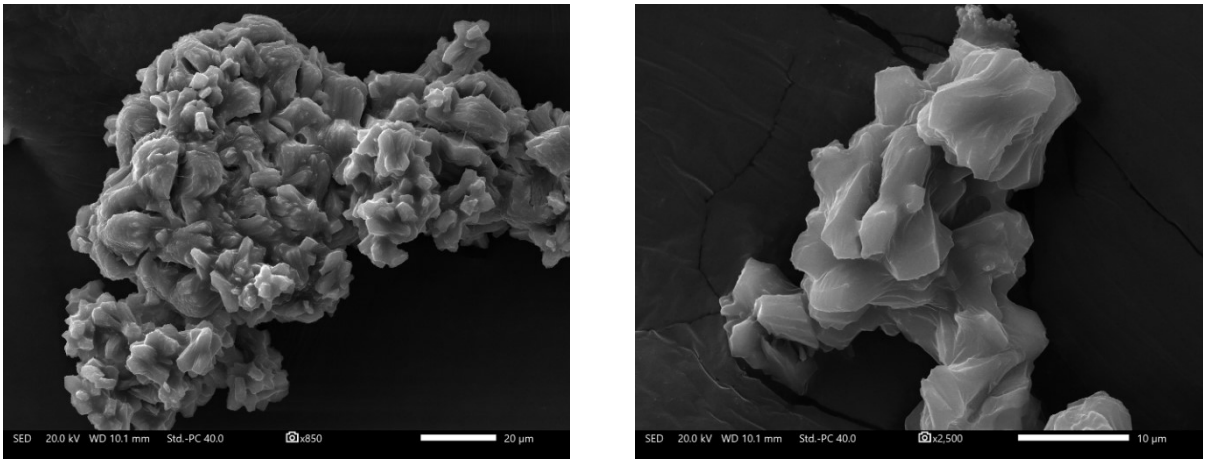

Figure S17. Scanning Electron Microscopy Images of Y-**stc**-MOF-1 crystals.

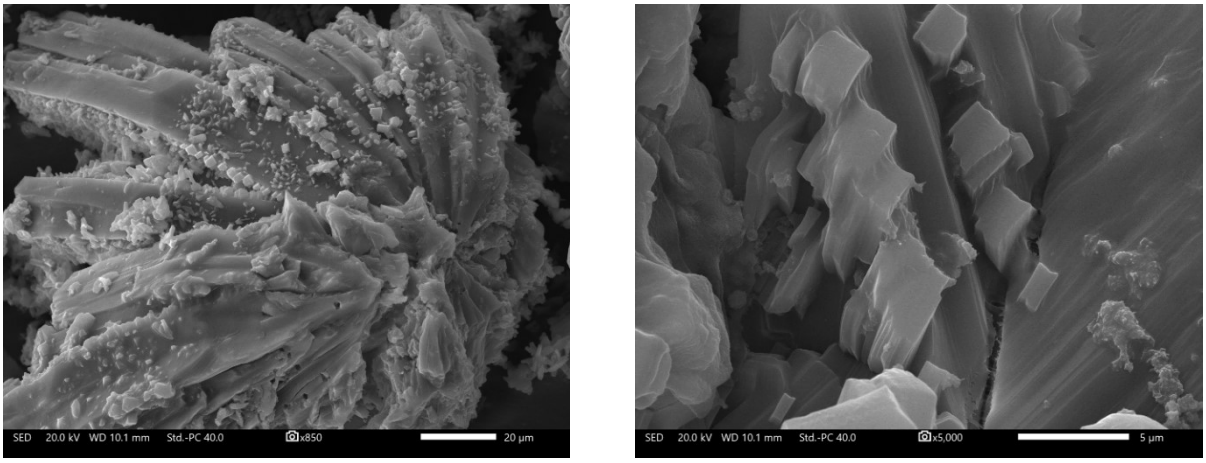

Figure S18. Scanning Electron Microscopy Images of Sm-**stc**-MOF-1 crystals.

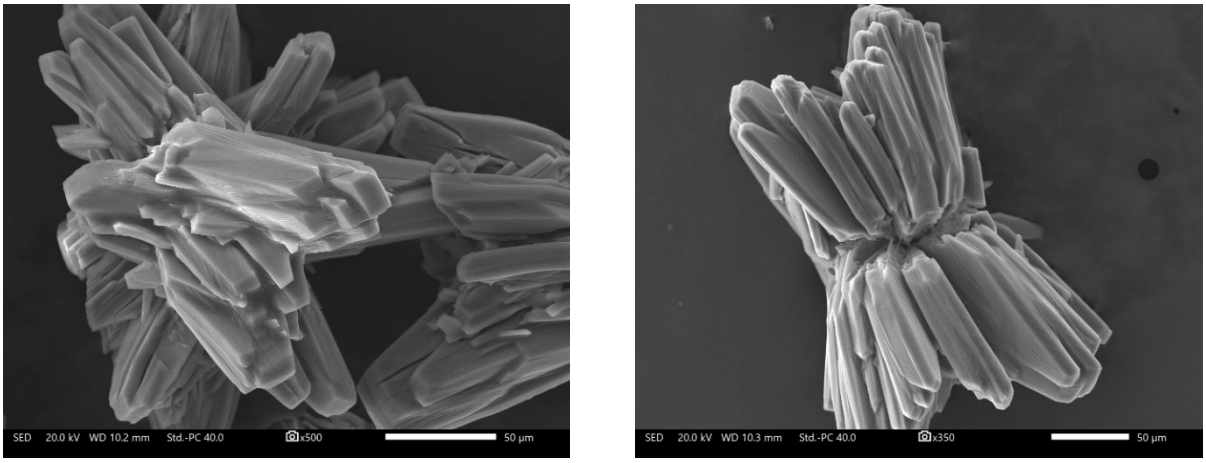

Figure S19. Scanning Electron Microscopy Images of Eu-**stc**-MOF-1 crystals.

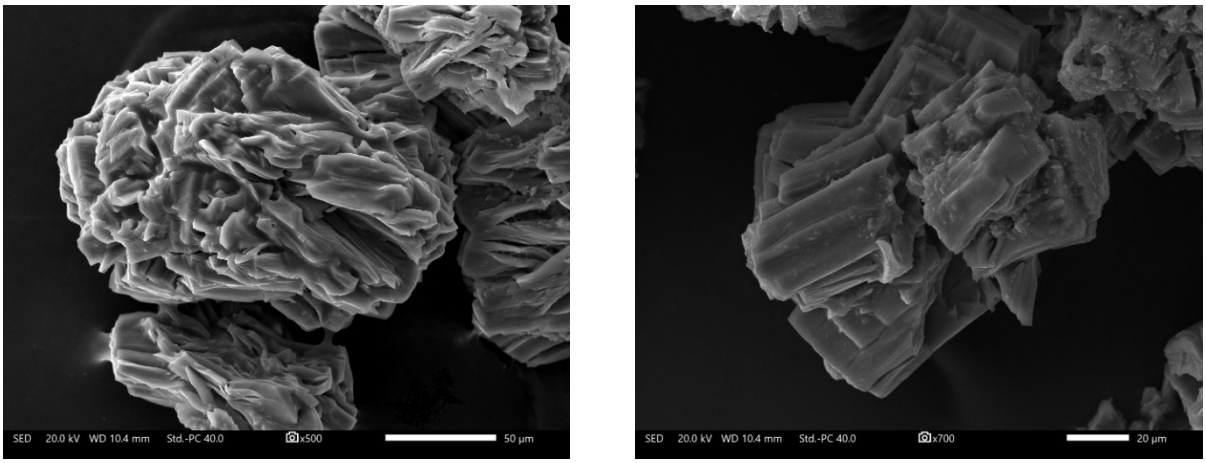

Figure S20. Scanning Electron Microscopy Images of Tb-**stc**-MOF-1 crystals.

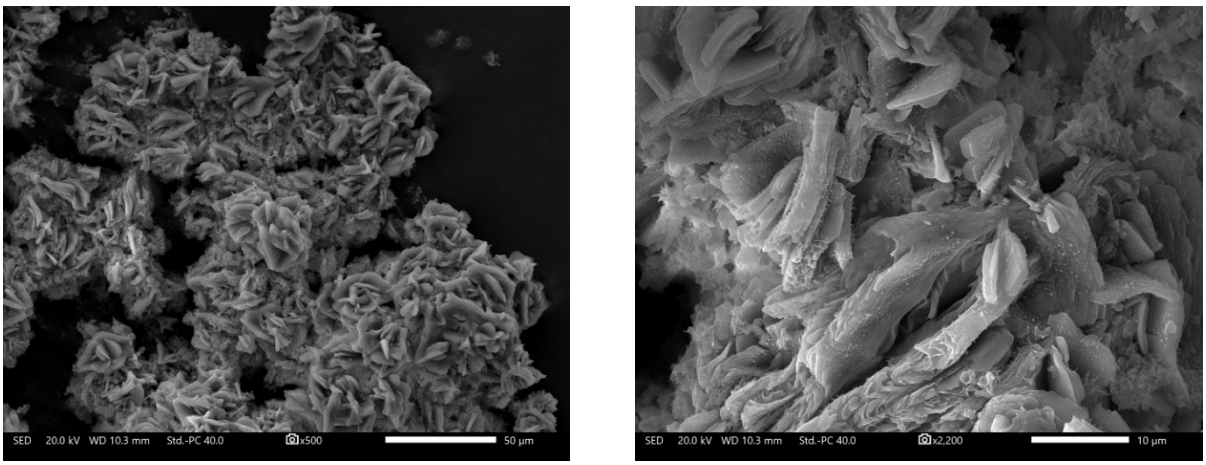

Figure S21. Scanning Electron Microscopy Images of Dy-**stc**-MOF-1 crystals.

Gas sorption measurements and analysis

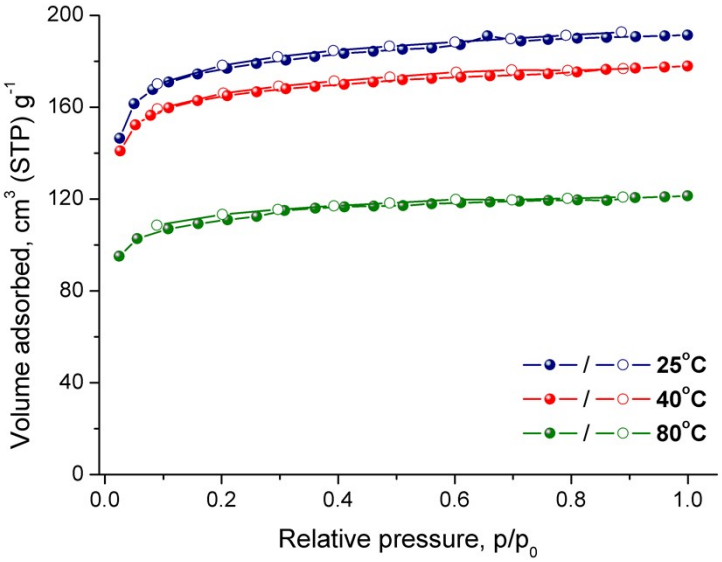

Figure S22. N_2 sorption isotherms of Tb-**stc**-MOF-1 recorded at 77 K, under different activation temperatures. Full and empty spheres indicate adsorption and desorption points, respectively.

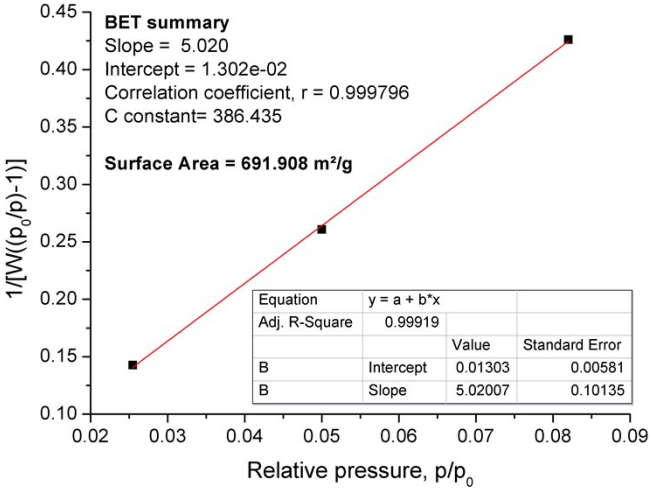

Figure S23. BET plot for Tb-**stc**-MOF-1 from the N_2 sorption isotherm recorded at 77 K (activation temperature: 25 °C).

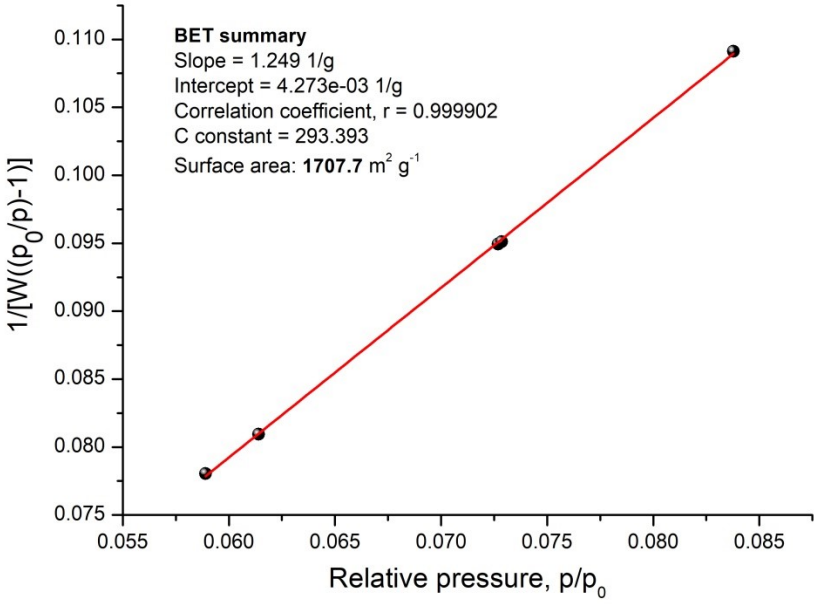

Figure S24. BET plot for Tb-**stc**-MOF-1 from the Ar sorption isotherm recorded at 87 K ($scCO_2$ activation).

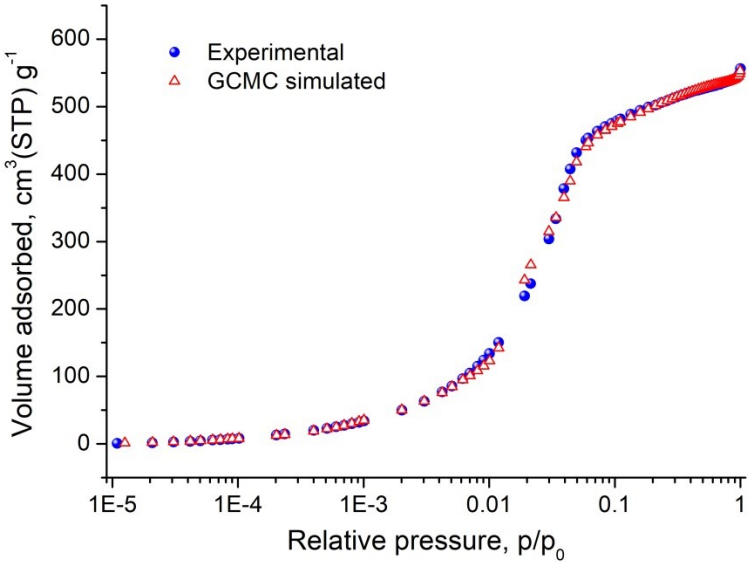

Figure S25. Simulation (red) of the experimental (blue) Ar sorption isotherm of Tb-**stc**-MOF-1 using the GCMC method provided by the BELMaster (TM) software from Microtrac.

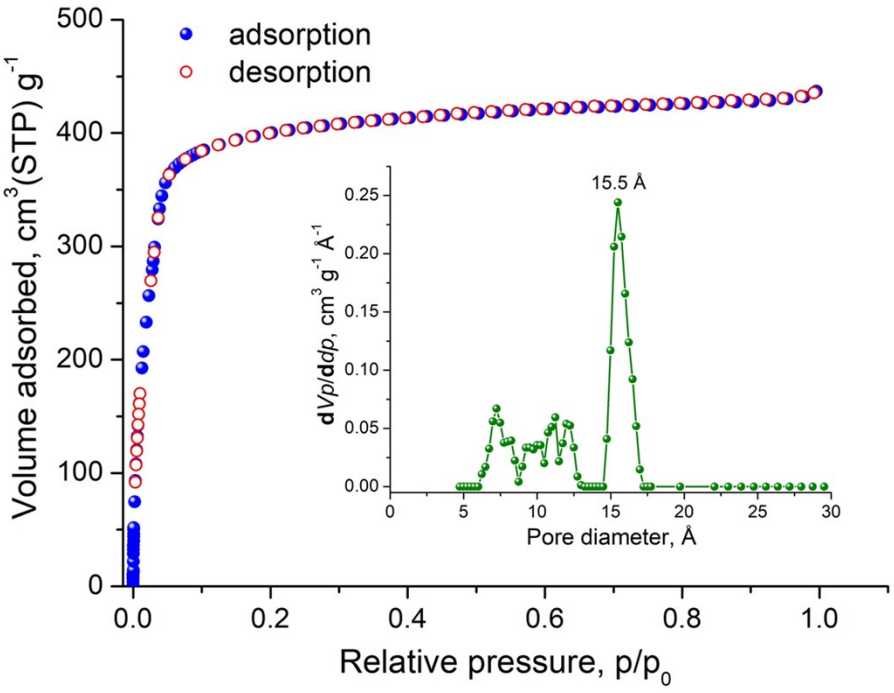

Figure S26. Argon sorption isotherm of activated Eu-**stc**-MOF-1 recorded at 87 K. Inset shows the corresponding pore size distribution curve obtained by GCMC method using the software BELMaster from Mircrotrac.

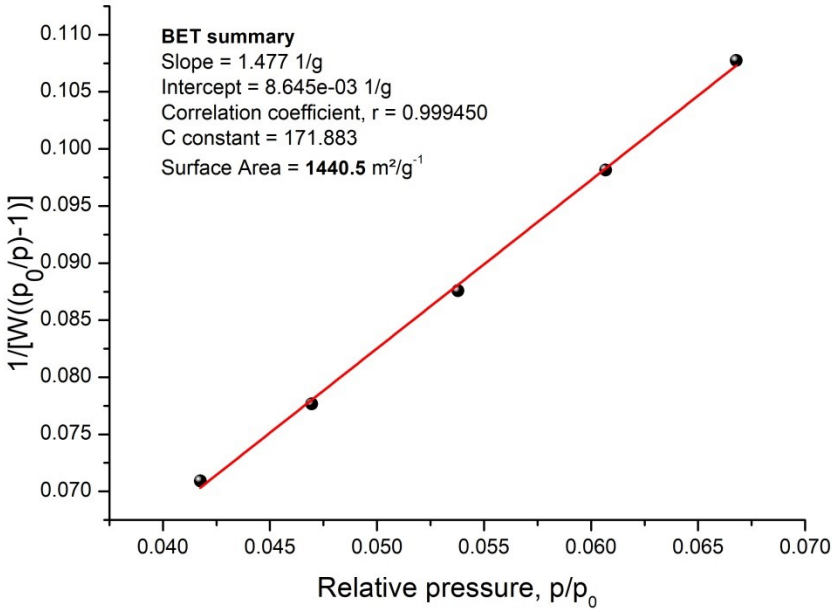

Figure S27. BET plot for Eu-**stc**-MOF-1 from the Ar sorption isotherm recorded at 87 K ($scCO_2$ activation).

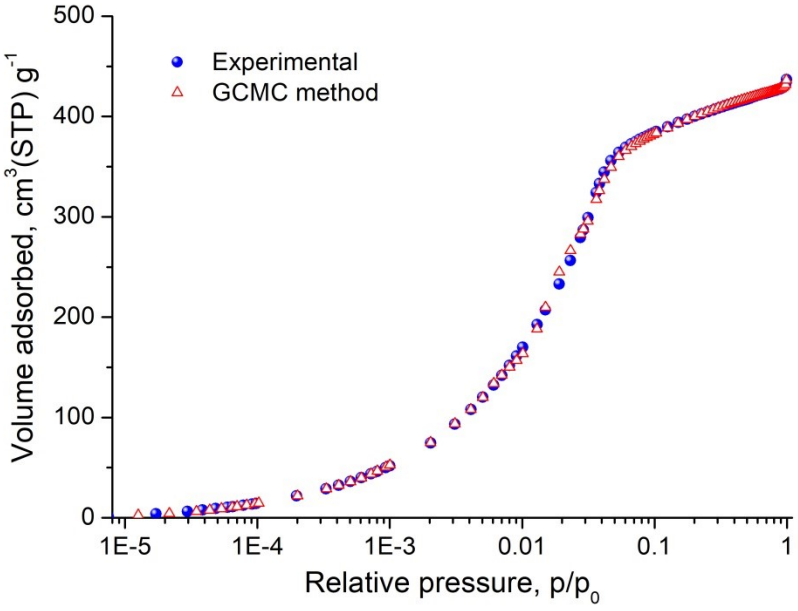

Figure S28. Simulation (red) of the experimental (blue) Ar sorption isotherm of Eu-**stc**-MOF-1 using the GCMC method provided by the BELMaster (TM) software from Microtrac.

Thermogravimetric analysis

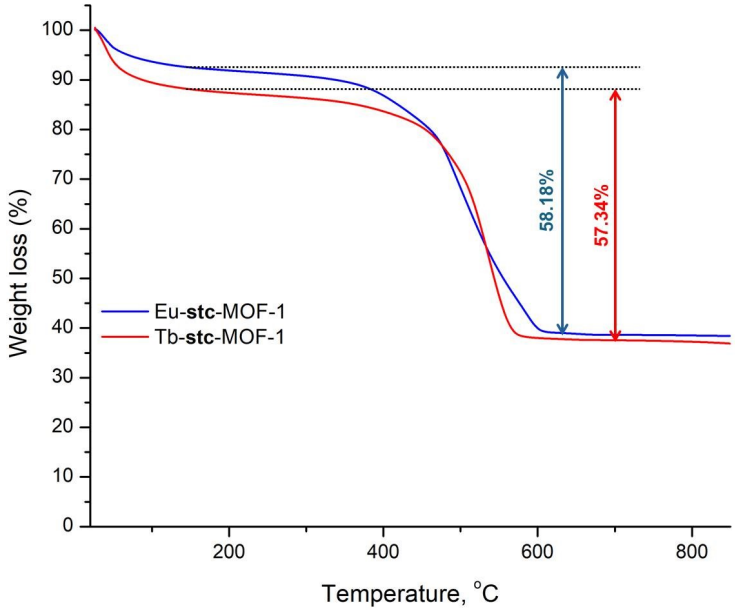

Figure S29. Thermogravimetric analysis curve of $scCO_2$ activated Tb-**stc**-MOF-1 and Eu-**stc**-MOF-1 recorded under nitrogen flow of 5 ml min^{-1}.

References

1 C. F. Macrae, P. R. Edgington, P. McCabe, E. Pidcock, G. P. Shields, R. Taylor, M. Towler and J. van De Streek, *J. Appl. Crystallogr.*, 2006, **39**, 453.

2 B. Liu, A. G. Wong-Foy and A. J. Matzger, *Chem. Commun.*, 2013, **49**, 1419.

3(a) G. K. Angeli, E. Loukopoulos, K. Kouvidis, A. Bosveli, C. Tsangarakis, E. Tylianakis, G. Froudakis and P. N. Trikalitis, *J. Am. Chem. Soc.*, 2021, **143**, 10250; (b) E. Loukopoulos, G. K. Angeli, K. Kouvidis, C. Tsangarakis and P. N. Trikalitis, *ACS Appl. Mater. Interfaces*, 2022, **14**, 22242.

4 Q. Hu, X. X. Tian, P. Wang, X. Y. Tang, W. H. Zhang and D. J. Young, *Inorg. Chem.*, 2021, **60**, 18614.

5 O. V. Dolomanov, A. J. Blake, N. R. Champness and M. Schroder, *J. Appl. Crystallogr.*, 2003, **36**, 1283.

6(a) G. M. Sheldrick, *Acta Crystallogr. Sect. A*, 2008, **64**, 112; (b) *Acta Crystallogr. Sect. A*, 2015, **71**, 3.

7 *Acta Crystallogr. Sect. C*, 2015, **71**, 3.

8(a) A. R. B. J. Lutton-Gething, B. F. Spencer, G. F. S. Whitehead, I. J. Vitorica-Yrezabal, D. Lee and M. P. Attfield, *Chem Mater*, 2024, **36**, 1957; (b) J. P. Vizuet, M. L. Mortensen, A. L. Lewis, M. A. Wunch, H. R. Firouzi, G. T. McCandless and K. J. Balkus, Jr., *J. Am. Chem. Soc.*, 2021, **143**, 17995.

9 A. L. Spek, *J. Appl. Crystallogr.*, 2003, **36**, 7.